

ABSTRACT

Background/aims: To investigate the characteristics of fundus autofluorescence (FAF) in acute Vogt-Koyanagi-Harada (VKH) disease.

Methods: FAF photography with blue light (BL-FAF) and near-infrared light (NIR-FAF) was performed on 10 eyes of 5 patients using a confocal scanning laser ophthalmoscope before and after treatment. The FAF images were followed for 6 months and retrospectively reviewed with comparisons of the other imaging modalities.

Results: At presentation, 4 eyes of 2 patients who presented soon after the initial ocular symptoms showed mild and uniform hyperautofluorescence in the macula mixed with hypoautofluorescence in the areas of serous retinal detachment. After immediate treatment with an intravenous high-dose steroid, the abnormal FAF returned to normal at 6 months. The other 6 eyes of 3 patients, who presented weeks after the symptoms, initially demonstrated diffuse and mottled hyperautofluorescence over the posterior pole, mixed with hypoautofluorescence induced by serous retinal detachment in 4 eyes. After treatment with an intravenous high-dose steroid, all 6 eyes showed scattered and widespread hyperautofluorescence, which gradually became evident and concentrated in the macula, partially resulting in some hypoautofluorescent dots at 6 months. The BL-FAF and the NIR-FAF demonstrated similar FAF patterns, but more evidently in NIR-FAF.

Conclusion: FAF photography noninvasively visualized sequential metabolic and functional changes in the retinal pigment epithelium (RPE) in acute VKH disease. The results suggest that early and sufficient treatment with a high-dose steroid might prevent persistent RPE damage. In addition, NIR-FAF can be an alternative method for the early detection of RPE abnormality.

Introduction

Vogt-Koyanagi-Harada (VKH) disease is a bilateral panuveitis accompanied by systemic disorders of the nervous, auditory, and integumentary systems.¹ In spite of diffuse choroidal inflammation, inflammatory cell infiltration is thought not to encroach into the choriocapillaris and the overlying retina.² However, the exudative retinal detachment and the pinpoint leakage on fluorescein angiography typically seen during the acute stage of VKH disease indicate alterations in the retinal pigment epithelium (RPE). In addition, chorioretinal depigmented lesions or RPE clumping are seen as the late manifestations of VKH disease.²⁻⁴ Therefore, subclinical stress on the RPE should be present in the course of VKH disease.

Fundus autofluorescence (FAF) photography with short wavelength light enables the visualization of lipofuscin in RPE and provides information about functional and metabolic changes in RPE. This method has been applied on various disorders involving RPE, such as age-related macular degeneration⁵⁻⁹ and central serous chorioretinopathy,¹⁰ as well as inflammatory disorders.^{11,12} Recent reports utilized near-infrared light for FAF photography and provided additional information for the characterization of several disease entities.¹³⁻¹⁶ Melanin, or melanin compounds, are thought to be the main source of FAF induced by near-infrared light, although some contributions from other possible fluorophores cannot be excluded.¹⁴ In this study, we investigated sequential changes in FAF characteristics in acute VKH disease before and after treatment by means of the two different wavelength lights.

Materials and Methods

In this study, the FAF images of 10 eyes of 5 patients with acute VKH disease seen at Kyoto Prefectural University of Medicine between April 2008 and September 2008 were retrospectively reviewed. The 5 patients consisted of 2 men and 3 women who were observed for at least 6 months before and after treatment at our hospital.

The diagnosis of VKH disease was made based on the revised diagnostic criteria.³ Serous retinal detachment documented as gradual dye pooling of subretinal fluid and optic nerve staining were revealed by fluorescein angiography.³ Indocyanine green (ICG) angiography was also performed before treatment and showed irregular and multifocal hypofluorescence, patchy or delayed filling, and indistinct choroidal vessels in the earlier phases with some hyperfluorescence over the posterior pole in the late phase.¹⁷⁻²⁰

All of the angiography and FAF photography were performed with a confocal scanning laser ophthalmoscope (Heidelberg Retina Angiograph 2, HRA2; Heidelberg Engineering, Heidelberg, Germany). Blue-light FAF (BL-FAF) photography was performed using a 30-degree field of view and 512 x 512 pixel resolution centered on the macula. The modality uses blue light at 488 nm for excitation and a barrier filter at 500 nm. In addition, near-infrared FAF (NIR-FAF) photography was performed with an excitation filter of 789 nm and a barrier filter of 800 nm normally used for ICG angiography. The best 9 and 15 images were taken and averaged to obtain a single image for BL-FAF and NIR-FAF, respectively; representative images of BL-FAF and NIR-FAF in a normal eye are shown in Figure 1. Optical coherence tomography (OCT) images were obtained with a time-domain OCT (Stratus OCT, version 4.0.1; Carl Zeiss Meditech, Inc., Dublin, CA) or a spectral-domain OCT (3D-OCT 1000 Mark II; Topcon Corp, Tokyo, Japan).

Results

All 10 eyes of the 5 patients presented with serous retinal detachment in the macula at the initial visit (figs 2, 4). The mean age of the 5 patients was 40 years. The clinical characteristics of the 5 patients are summarized in Table 1.

Table 1. Characteristics of the Patients with Acute Vogt-Koyanagi-Harada Disease

Case No.	Gender /Age	Eye	Duration from Onset to Steroid Pulse	Abnormal FAF at Initial Visit	Abnormal FAF at Month 1	Abnormal FAF at Month 6	BCVA at Initial Visit (Decimal)	BCVA at Month 6 (Decimal)
1	F/16	R	4 Days	+	+	-	0.6	1.5
		L		+	+	-	1.0	1.5
2	M/19	R	4 Days	+	+	-	0.04	1.5
		L		+	+	-	0.04	1.5
3	F/53	R	4 Weeks	+	+	+	0.7	0.6
		L		+	+	+	0.4	0.6
4	F/40	R	7 Weeks	+	+	+	1.0	0.9
		L		+	+	+	1.2	0.9
5	M/74	R	3 Weeks	+	+	+	0.2	0.8
		L		+	+	+	0.3	0.8

BCVA, best corrected visual acuity; F, female; FAF, fundus autofluorescence; L, left eye; M, male; R, right eye

In accordance with the revised criteria for VKH disease established by the International Nomenclature Committee,³ all 5 patients were classified as incomplete VKH.

Of these 5 patients, 2 patients (Cases 1 and 2) presented to our hospital immediately after the ocular symptoms. Two patients (Cases 3 and 4) were insufficiently treated with low-dose oral prednisolone for 4 and 7 weeks, respectively, before the initial visit to our hospital. The other patient (Case 5) received no treatment for 3 weeks after the initial ocular symptoms.

All 5 patients were hospitalized at our hospital soon after the initial visit, and were treated with steroid pulse (intravenous drip infusion of 1000 mg methylprednisolone/day for 3 consecutive days) followed by a 50- to 60-mg daily dose of oral prednisolone, resulting in complete resolution of the retinal detachment within 2 weeks. The dose of oral prednisolone was gradually tapered over more than 6 months.

Four eyes of 2 patients (Cases 1 and 2), who had undergone steroid pulse immediately after the onset of ocular symptoms, demonstrated mild and uniform hyperautofluorescence in the macula mixed with hypoautofluorescence inside, but not in all areas of the serous retinal detachment at the initial visit, particularly in NIR-FAF (fig 3A,B). That hyperautofluorescence was seen in the areas of irregular hypofluorescence in the macula observed on ICG angiography, but the multifocal hypofluorescence on ICG angiography was more numerous and more extensively observed (fig 2D). After resolution of the serous retinal detachment, the hyperautofluorescence remained for at least 1 month after steroid pulse, wider and more clearly in NIR-FAF than in BL-FAF (fig 3C,D). With time, the hyperautofluorescence in the macula decreased in both size and intensity, and there appeared to be no abnormal FAF at 6 months after steroid pulse (fig 3E,F). OCT did not show any abnormalities at 6 months (fig 3H).

Six eyes of the other 3 patients (Cases 3, 4, and 5), who had not undergone steroid pulse until 3 to 7 weeks after the onset of the ocular symptoms, initially showed diffuse and mottled hyperautofluorescence over the posterior pole, more clearly demonstrated in NIR-FAF (fig 5A,B). In addition, 4 eyes of 2 patients (Cases 4 and 5) demonstrated hypoautofluorescence in the areas of serous retinal detachment, but 2 eyes of 1 patient (Case 3) showed no hypoautofluorescence in spite of the retinal detachment. After resolution of the retinal detachment, all 6 eyes gradually showed placoid hyperautofluorescence in the macula, and surrounding scattered hyperautofluorescence accompanied by radial patterns of hyperautofluorescence around the optic disc (fig 5C,D).

That hyperautofluorescence corresponded to irregular and multifocal hypofluorescence on ICG angiography, but the hypofluorescent spots on ICG angiography were more numerous and extensive. The radial hyperautofluorescence appeared to be consistent with choroidal folds seen in the angiograms (figs 4D and 5C,D).²¹ The pattern of hyperautofluorescence in NIR-FAF was similar to that in BL-FAF, but more evident in NIR-FAF. Such hyperautofluorescence in BL-FAF and NIR-FAF gradually decreased in size, yet contrary to Case 1 and Case 2, increased in intensity in the fovea, showing granular hyperautofluorescence with some hypoautofluorescent dots surrounded by larger placoid hyperautofluorescence at 6 months (fig 5E,F). Some areas of that granular hyperautofluorescence in the fovea appeared to correspond to yellowish or punctate pigmentary dots at the level of the RPE seen in the color photographs (fig 5G), but the distribution of the granular hyperautofluorescence was more widespread. In 1 patient (Case 5), the choroidal inflammation relapsed two times in conjunction with the choroidal folds (at 3 months and 5 months after steroid pulse), but the BL-FAF and the NIR-FAF did not change before and after the recurrent episodes. OCT showed multifocal thickening of the RPE monolayer, some of which was consistent with granular hyperautofluorescence in the fovea (fig 5I). In the areas of placoid hyperautofluorescence, the OCT showed defects in the boundary between the photoreceptor inner and outer segments (IS/OS) with no RPE abnormality (fig 5H).

Discussion

This study investigated 10 eyes of 5 patients with acute VKH disease, and demonstrated their sequential changes in FAF. We found that the abnormal FAF occasionally persisted at 6 months after steroid therapy even after complete resolution of exudative retinal detachment in patients who received late effective steroid treatment.

The FAF patterns after the resolution of retinal detachment seen in this study can be divided into 2 patterns. The first pattern was seen in the patients who had undergone immediate intensive treatment with steroid pulse and showed mild hyperautofluorescence during the early phase of the disease. The hyperautofluorescence then decreased in size and intensity with time, resulting in normal FAF at 6 months. The second pattern was seen in the patients who had not undergone immediate treatment with steroid pulse and showed scattered and widespread hyperautofluorescence during the early phase. The hyperautofluorescence concentrated centripetally with time, resulting in some

hyperautofluorescent dots mixed with hypoautofluorescent dots more evident in NIR-FAF than in BL-FAF at 6 months. Previous studies have found that the interval between the development of ocular symptoms and treatment seemed to be an important predictor for visual outcome.^{22,23} Early and sufficient treatment with a high-dose steroid may be important to protect the RPE from metabolic and functional stress and preserve the visual function. FAF photography longitudinally enabled the visualization of such stress on the RPE.

In this study, we used NIR-FAF photography in addition to the conventional BL-FAF photography. This method was recently introduced,^{13,14} and is thought to visualize oxidized melanin or compounds closely associated with melanin.¹⁴ Although the BL-FAF has been applied to many posterior diseases, the absorption of the short wavelength light by the macular pigment often obscures the precise condition of the RPE in the macula. In this study, the NIR-FAF showed similar patterns to the BL-FAF, but more evidently in the NIR-FAF. The NIR-FAF is known to originate in part from the RPE,¹⁴ and it is not blocked by the macular pigment. Therefore, the NIR-FAF may have potential to be an alternative method for detection of early RPE disturbance seen in acute VKH disease, as well as other posterior diseases.^{15,16}

Although our study included a small number of patients, comparisons between FAF photography and the other imaging modalities indicates some implications. The hyperautofluorescence seen in the early course of the disease corresponded to irregular and multifocal hypofluorescence on ICG angiography. Such hypofluorescence on ICG angiography is thought to represent the choroidal inflammatory foci in acute VKH disease,¹⁷ suggesting that choroidal inflammation affected the RPE metabolism in all 5 cases. However, early treatment with a high-dose steroid might have prevented the persistent damage in Case 1 and Case 2. On the other hand, the 3 cases treated late after the onset of symptoms showed a gradual concentration of abnormal FAF in the macula, exhibiting granular hyperautofluorescence and hypoautofluorescence in the central part surrounded by placoid hyperautofluorescence at 6 months. As shown in Figure 4, the areas of placoid hyperautofluorescence showed a normal RPE monolayer with the defect of IS/OS in OCT, thus suggesting that there was RPE dysfunction affecting the photoreceptor layer. The central granular hyperautofluorescence corresponded in part to multifocal thickening of the RPE monolayer visualized in OCT and to yellowish granules or pigmentary dots seen in the color photographs. Future studies using higher-resolution OCT

may clarify the precise relationship between the morphologic alterations and the FAF findings.

It should be noted that this study has limitations due to the small number of patients and the limited follow-up period. In addition, retrospective design did not allow us to show more detailed correlation between the FAF photography and the other imaging modalities. We also acknowledge that our results might have been influenced by other factors such as age, since a younger age at onset was found to be a prognostic factor for better visual outcome.²³⁻²⁵ However, and to the best of our knowledge, this is the first study to demonstrate the sequential changes in FAF and provide information about the condition of the RPE in acute VKH disease. It remains unclear at this point whether adjusting the dosage of the oral steroid treatment or other immunosuppressive agents following the initial immediate and sufficient treatment with a high-dose steroid can alter the course of the abnormal FAF and visual outcome. Future studies are required to elucidate this matter.

Competing interests: None

Ethics approval: Approval from the institutional review board was not required for this retrospective study.

Patient consent: Informed consent was obtained from all of the patients prior to initiation of this retrospective study.

The Corresponding Author has the right to grant on behalf of all authors and does grant on behalf of all authors, an exclusive licence (or non-exclusive for government employees) on a worldwide basis to the BMJ Publishing Group Ltd and its Licensees to permit this article (if accepted) to be published in the British Journal of Ophthalmology and any other BMJ PGL products to exploit all subsidiary rights, as set out in our licence (<http://bjo.bmj.com/ifora/licence.pdf>).

Figure Legends

Figure 1

The healthy right eye of a 32-year-old male. The blue-light fundus autofluorescence (BL-FAF) photography (A) and the near-infrared FAF (NIR-FAF) photography (B) demonstrated hypoautofluorescence caused by the major retinal vessels and the optic disc. In the BL-FAF photography, the FAF from the central fovea is obscured by the macular pigment which absorbs short-wave-length light, whereas the NIR-FAF showed subtle hyperautofluorescence in the central macula.

Figure 2

Case 1. A 16-year-old woman with acute Vogt-Koyanagi-Harada (VKH) disease. This patient presented to our hospital the day after her initial ocular symptoms. (A) The left eye showed multilobular serous retinal detachment in the macula. (B) Optical coherence tomography (OCT) (the location is indicated with arrow in (A)) demonstrated elevation of the neurosensory retina with accumulation of subretinal fluid. The fluorescein angiogram (C) showed multiple pinpoint leakages in the macula. The middle phase of indocyanine green (ICG) angiography (D) demonstrated numerous and extensive hypoautofluorescent spots (arrows) observed in more confluent and irregular form in the macula (arrowheads). Some parts of the highly elevated retinal detachment were also visualized as hypofluorescence (asterisks).

Figure 3

Case 1 (Cont.). At the initial visit, the BL-FAF (A) and the NIR-FAF (B) demonstrated mild and uniform hyperautofluorescence in the macula, but some parts of the serous retinal detachment (See fig 2D, asterisks) caused hypoautofluorescence. At 1 month after the steroid pulse, the BL-FAF (C) showed subtle hyperautofluorescence (arrows) around the central fovea, whereas the NIR-FAF (D) showed wider and more evident hyperautofluorescence in the macula (arrows). At 6 months, the BL-FAF (E) and the NIR-FAF (F) returned to normal. The color photograph (G) and the OCT (H, the location is indicated with an arrow in (G)) at 6 months showed no abnormal findings. Arrowheads in (G) indicate the intact boundary between the photoreceptor inner and outer segments (IS/OS).

Figure 4

Case 3. A 53-year-old woman who had not undergone immediate steroid pulse for 4 weeks. The left eye (A) initially showed serous retinal detachment in the macula evidenced by OCT (B)(the location is indicated by arrow in (A)). Fluorescein angiography (C) demonstrated diffuse dye leakage over the posterior pole and optic nerve staining. The middle phase of ICG angiography (D) revealed numerous hypofluorescent spots (arrows), which were observed in confluent and irregular form in the central macula. Note that there are radial patterns of hypofluorescence representing choroidal folds (yellow arrowheads).

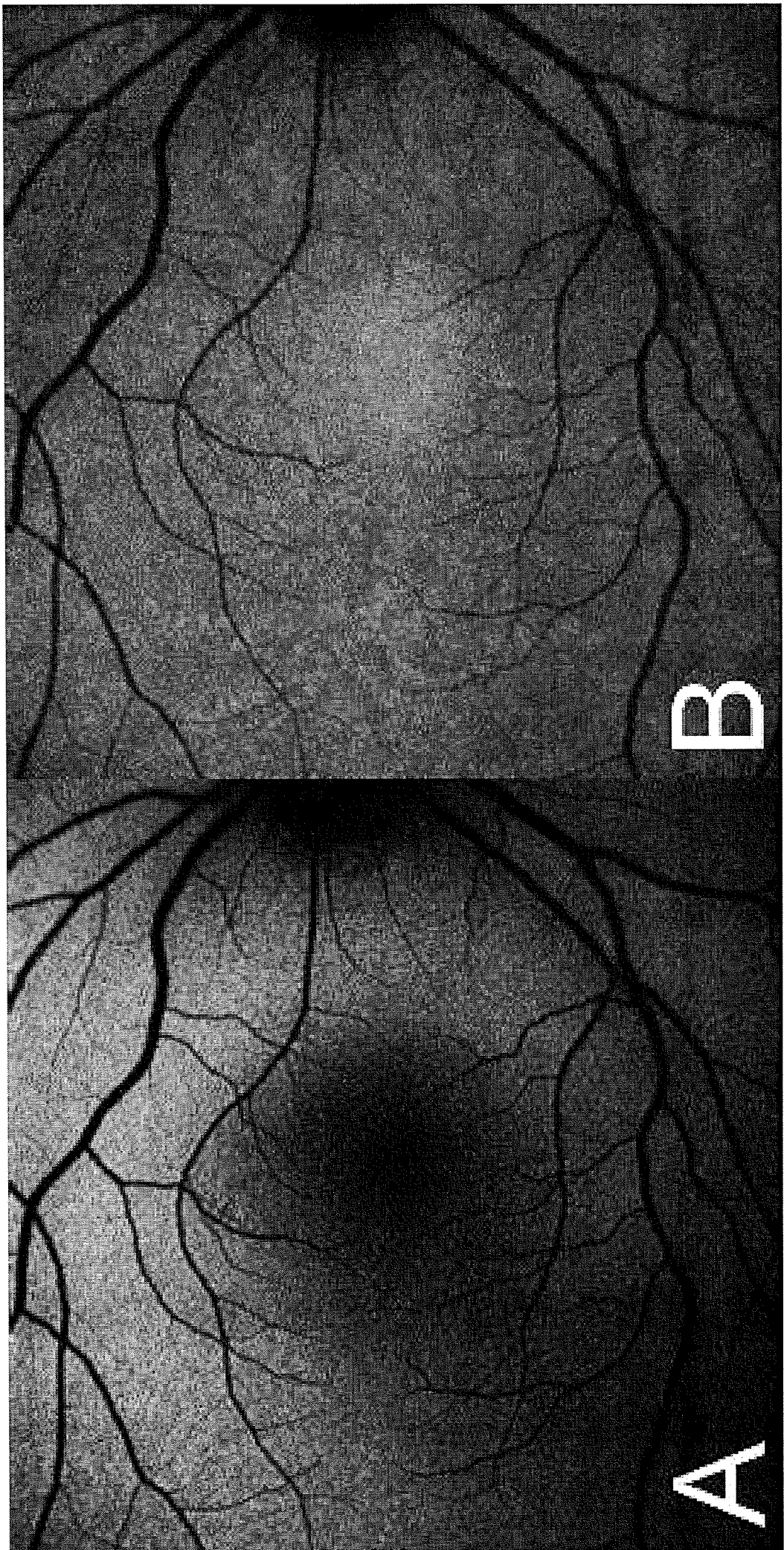
Figure 5

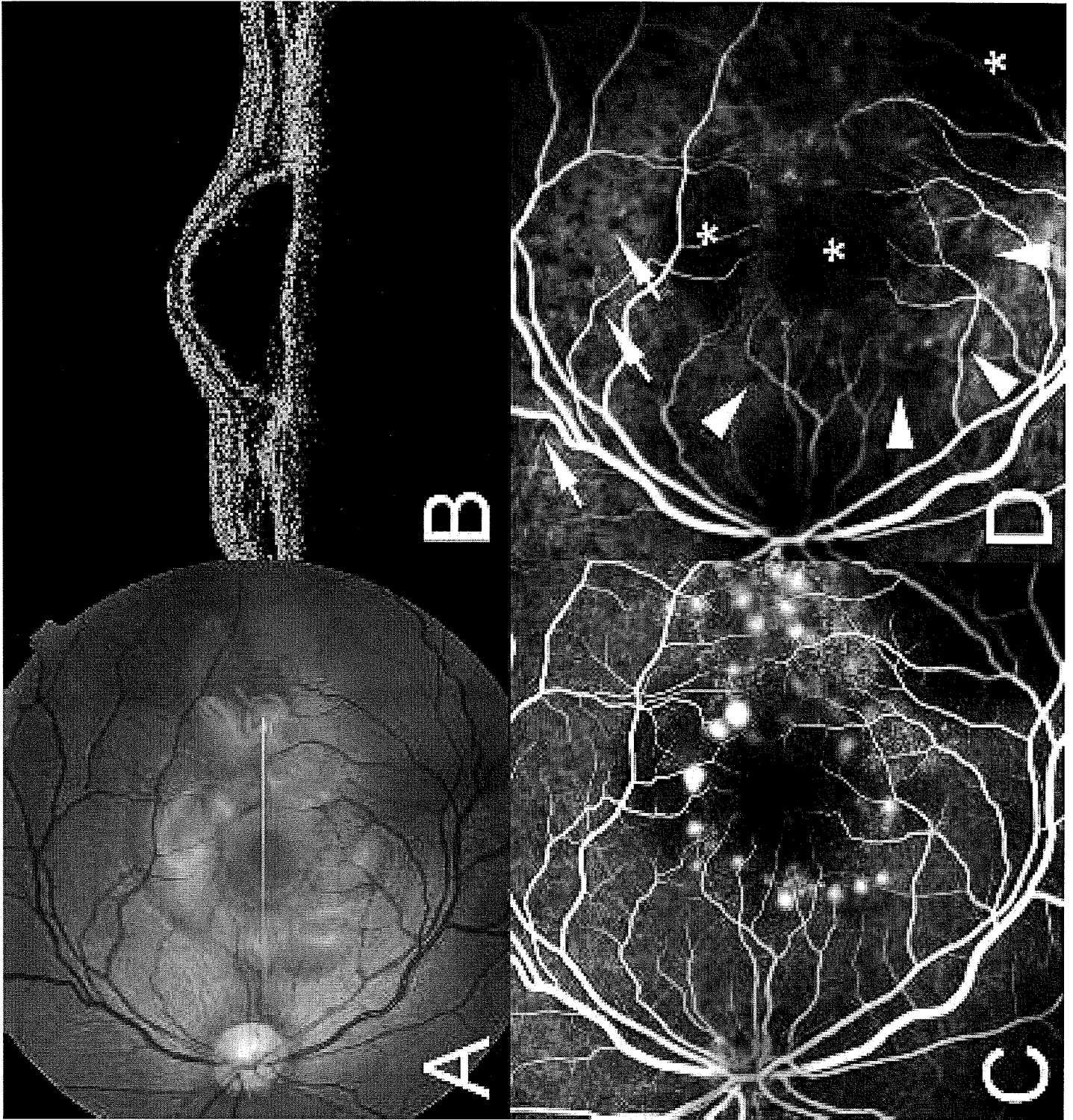
Case 3 (Cont.). At the initial visit, the BL-FAF (A) and the NIR-FAF (B) demonstrated diffuse and mottled hyperautofluorescence over the posterior pole, but the intensity was weak. At 1 month after the steroid pulse, the BL-FAF (C) and the NIR-FAF (D) showed placoid and scattered hyperautofluorescence in the macula in association with radial hyperautofluorescence around the optic disc (yellow arrowheads). At 6 months, the BL-FAF (E) and the NIR-FAF (F) demonstrated granular hyperautofluorescence in the fovea and surrounding placoid FAF, more evidently demonstrated in NIR-FAF. Note that there appeared to be some hypoautofluorescent dots (E, F, arrows) in the fovea. The color photograph at 6 months (G) demonstrates some yellowish granules and pigmentary dots in the fovea. OCT (the locations are indicated with arrows in (G)) showed normal hyperreflective RPE monolayer and defect in the IS/OS in the area of placoid hyperautofluorescence (H), whereas it demonstrated multifocal thickening of the RPE line (I, arrows) with intact IS/OS boundary (I, arrowheads).

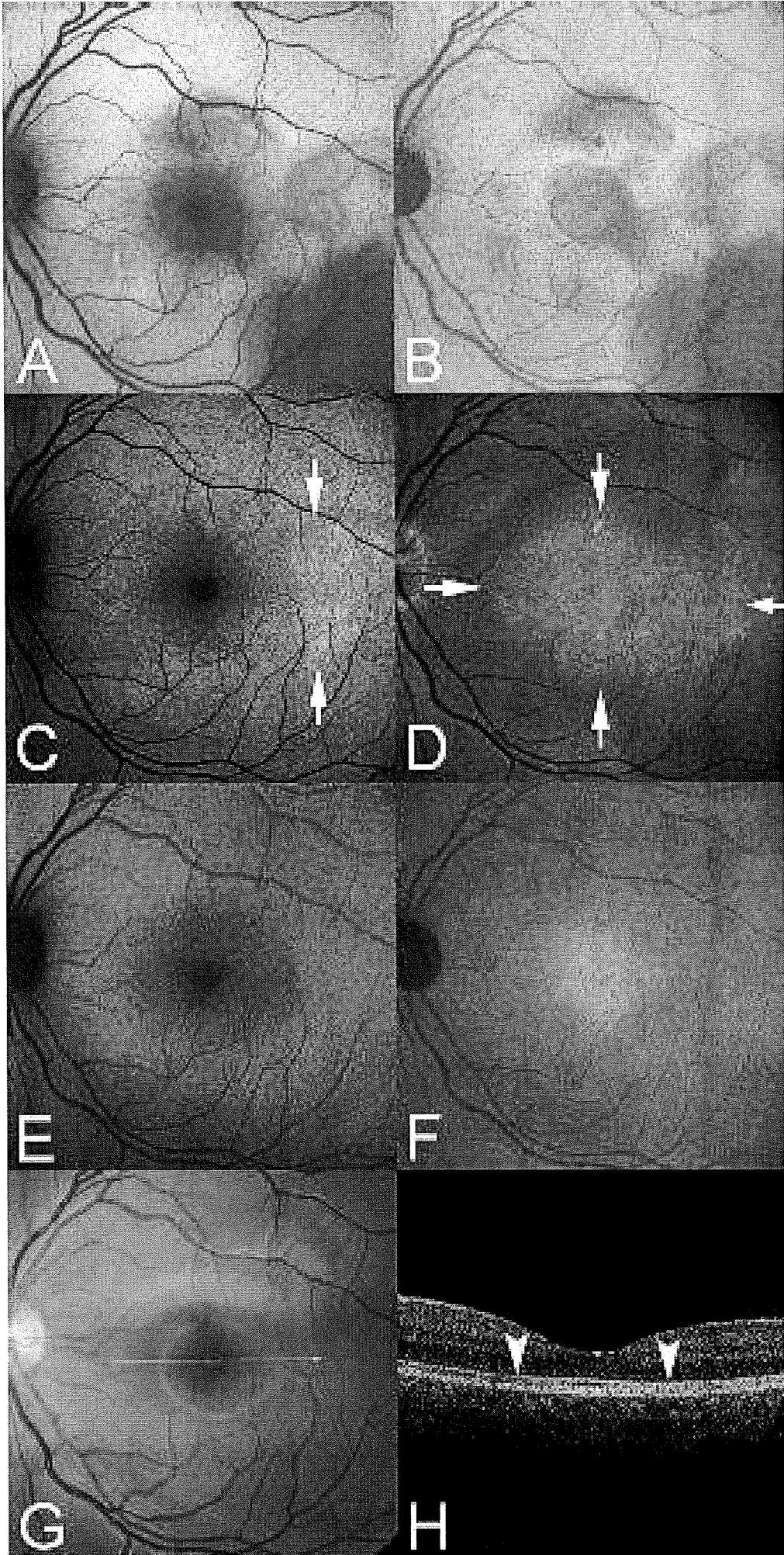
References

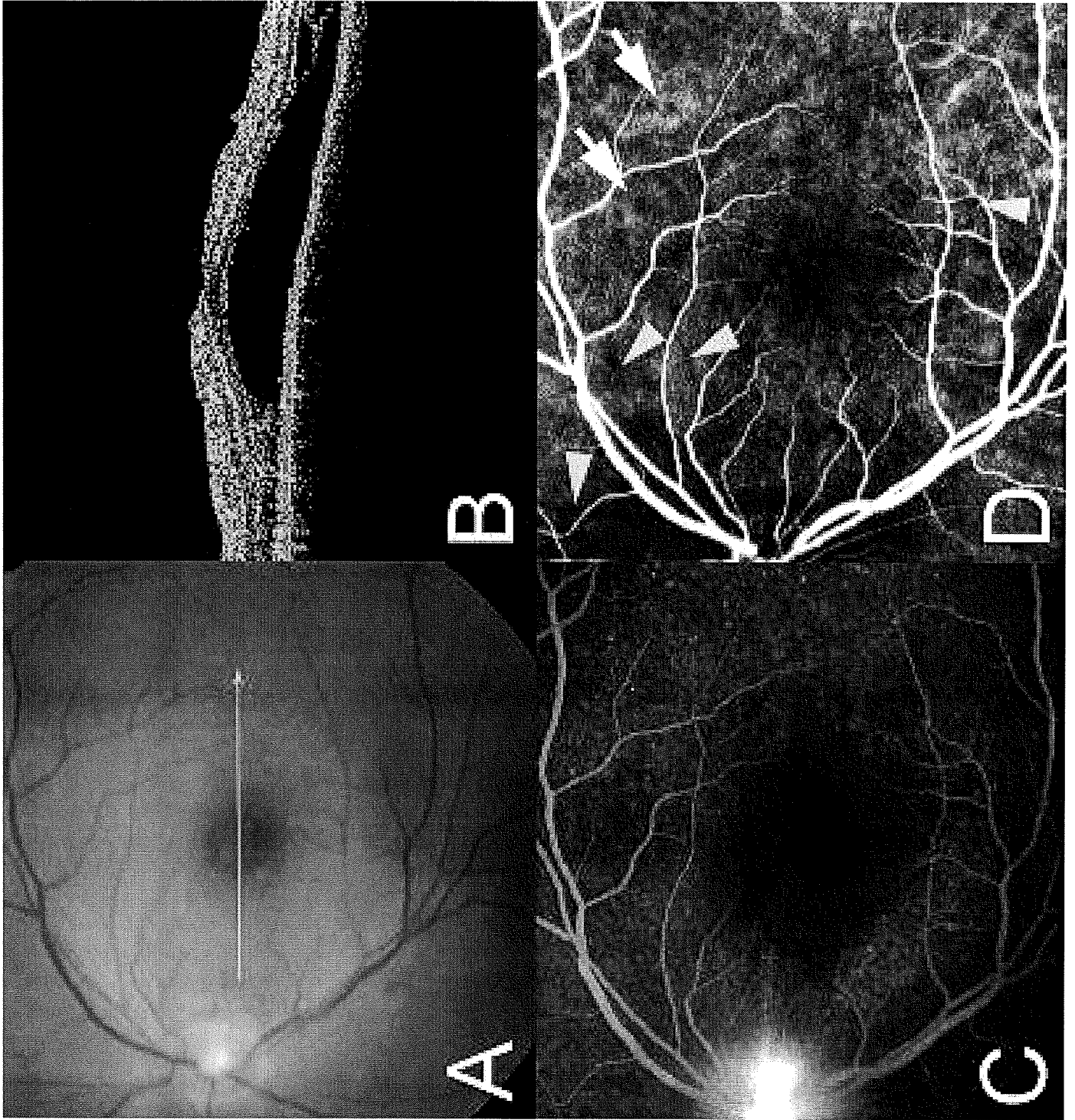
1. Moorthy RS, Inomata H, Rao NA. Vogt-Koyanagi-Harada syndrome. *Surv Ophthalmol* 1995;39:265-292.
2. Rao NA. Pathology of Vogt-Koyanagi-Harada disease. *Int Ophthalmol*. 2007;27:81-85.
3. Read RW, Holland GN, Rao NA, et al. Revised diagnostic criteria for Vogt-Koyanagi-Harada disease: report of an international committee on nomenclature. *Am J Ophthalmol* 2001;131:647-652.
4. Inomata H, Rao NA. Depigmented atrophic lesions in sunset glow fundi of Vogt-Koyanagi-Harada disease. *Am J Ophthalmol* 2001;131:607-614.
5. Holz FG, Bindewald-Wittich A, Fleckenstein M, Dreyhaupt J, Scholl HP, Schmitz-Valckenberg S. Progression of geographic atrophy and impact of fundus autofluorescence patterns in age-related macular degeneration. *Am J Ophthalmol* 2007;143:463-472.
6. Spaide RF. Fundus autofluorescence and age-related macular degeneration. *Ophthalmology* 2003;110:392-399.
7. Vaclavik V, Vujosevic S, Dandekar SS, Bunce C, Peto T, Bird AC. Autofluorescence imaging in age-related macular degeneration complicated by choroidal neovascularization: a prospective study. *Ophthalmology* 2008;115:342-346.
8. McBain VA, Townend J, Lois N. Fundus autofluorescence in exudative age-related macular degeneration. *Br J Ophthalmol* 2007;91:491-496.
9. Hwang JC, Chan JW, Chang S, Smith RT. Predictive value of fundus autofluorescence for development of geographic atrophy in age-related macular degeneration. *Invest Ophthalmol Vis Sci* 2006;47:2655-2661.
10. Spaide RF, Klancnik JM, Jr. Fundus autofluorescence and central serous chorioretinopathy. *Ophthalmology* 2005;112:825-833.
11. Koizumi H, Pozzoni MC, Spaide RF. Fundus autofluorescence in birdshot chorioretinopathy. *Ophthalmology* 2008;115:e15-20.
12. Haen SP, Spaide RF. Fundus autofluorescence in multifocal choroiditis and panuveitis. *Am J Ophthalmol* 2008;145:847-853.
13. Weinberger AW, Lappas A, Kirschkamp T, et al. Fundus near infrared fluorescence correlates with fundus near infrared reflectance. *Invest Ophthalmol Vis Sci* 2006;47:3098-3108.

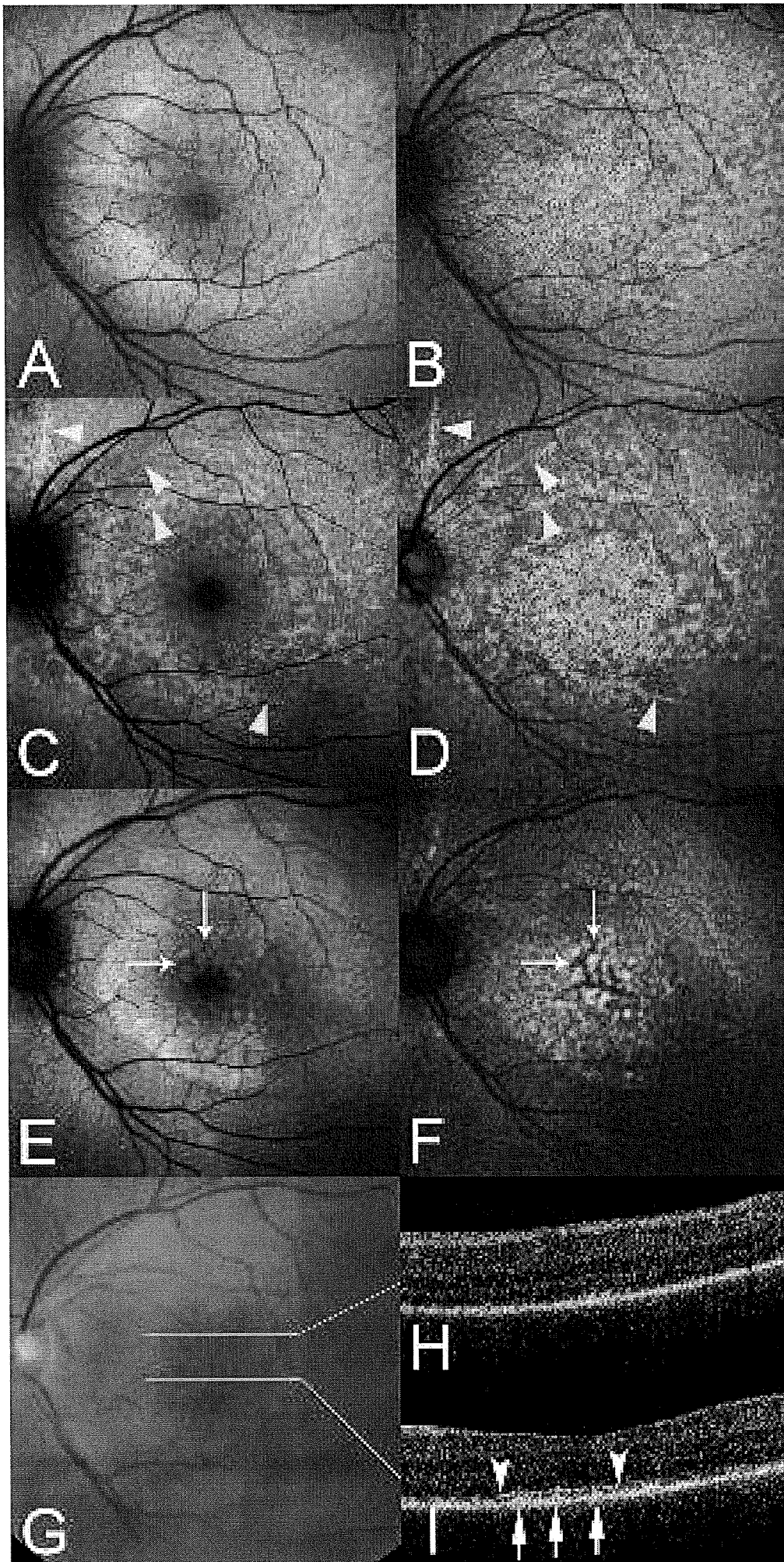
14. Keilhauer CN, Delori FC. Near-infrared autofluorescence imaging of the fundus: visualization of ocular melanin. *Invest Ophthalmol Vis Sci* 2006;47:3556-3564.
15. Parodi MB, Iacono P, Pedio M, et al. Autofluorescence in adult-onset foveomacular vitelliform dystrophy. *Retina* 2008;28:801-807.
16. Ayata A, Tatlipinar S, Kar T, Unal M, Ersanli D, Bilge AH. Near-infrared and short-wavelength autofluorescence imaging in central serous chorioretinopathy. *Br J Ophthalmol* 2009;93:79-82.
17. Bouchenaki N, Herbort CP. The contribution of indocyanine green angiography to the appraisal and management of Vogt-Koyanagi-Harada disease. *Ophthalmology* 2001;108:54-64.
18. Kohno T, Miki T, Shiraki K, et al. Subtraction ICG angiography in Harada's disease. *Br J Ophthalmol* 1999;83:822-833.
19. Okada AA, Mizusawa T, Sakai J, Usui M. Videofunduscopy and videoangiography using the scanning laser ophthalmoscope in Vogt-Koyanagi-Harada syndrome. *Br J Ophthalmol* 1998;82:1175-1181.
20. Oshima Y, Harino S, Hara Y, Tano Y. Indocyanine green angiographic findings in Vogt-Koyanagi-Harada disease. *Am J Ophthalmol* 1996;122:58-66.
21. Wu W, Wen F, Huang S, Luo G, Wu D. Choroidal folds in Vogt-Koyanagi-Harada disease. *Am J Ophthalmol* 2007;143:900-901.
22. Sheu SJ, Kou HK, Chen JF. Prognostic factors for Vogt-Koyanagi-Harada disease. *J Chin Med Assoc* 2003;66:148-154.
23. Chee SP, Jap A, Bacsal K. Prognostic factors of Vogt-Koyanagi-Harada disease in Singapore. *Am J Ophthalmol* 2009;147:154-161, e151.
24. Read RW, Rechodouni A, Butani N, et al. Complications and prognostic factors in Vogt-Koyanagi-Harada disease. *Am J Ophthalmol* 2001;131:599-606.
25. Al-Kharashi AS, Aldibhi H, Al-Fraykh H, Kangave D, Abu El-Asrar AM. Prognostic factors in Vogt-Koyanagi-Harada disease. *Int Ophthalmol* 2007;27:201-210.











Cultivated Human Conjunctival Epithelial Transplantation for Total Limbal Stem Cell Deficiency

Leonard P. K. Ang,^{1,2,3,4,5} Hidetoshi Tanioka,^{3,5} Satoshi Kawasaki,³ Leslie P. S. Ang,⁶ Kenta Yamasaki,³ Tien Phuc Do,⁷ Zaw M. Thein,⁷ Noriko Koizumi,³ Takahiro Nakamura,³ Norihiko Yokoi,³ Aoi Komuro,³ Tsutomu Inatomi,³ Mina Nakatsukasa,³ and Shigeru Kinoshita³

PURPOSE. To determine the feasibility of cultivated conjunctiva as a viable epithelial sheet for transplantation and corneal resurfacing in eyes with limbal stem cell deficiency (LSCD).

METHODS. Human corneal epithelial (HCE) and human conjunctival epithelial (HCjE) cells were cultivated on human amniotic membrane (AM) to confluence and then air lifted to allow further stratification and differentiation. Denuded AM and cultivated HCE and cultivated HCjE cells were then transplanted into 18 eyes of rabbits with induced LSCD. The cultivated and engrafted epithelia were examined by transmission electron microscopy (TEM) and immunohistochemistry. Two weeks after transplantation, the eyes were examined by slit lamp biomicroscopy and scored on epithelial integrity, corneal haze, and corneal neovascularization.

RESULTS. Both cultivated and engrafted HCjE sheets demonstrated confluent epithelial sheets with five to six layers of well-stratified epithelium. TEM examination of engrafted HCjE revealed numerous microvilli, desmosomes, and hemidesmosomes, identical with in vivo corneal epithelium. Immunohistochemical analysis of both HCjE and HCE cells showed the presence of CK3, CK4, and CK12, with absence of Muc5AC. Clinical outcomes for eyes receiving HCjE transplants and HCE transplants were comparable, with most having transparent, smooth corneas, free of epithelial defects.

CONCLUSIONS. The study showed that microscopically, HCjE cells have features similar to HCE cells, with clinically equivalent outcomes. The ex vivo cultivation of conjunctiva to form transplantable epithelial sheets for corneal replacement is a

promising new treatment modality in patients with LSCD. (*Invest Ophthalmol Vis Sci.* 2010;51:758-764) DOI:10.1167/iov.09-3379

The ocular surface forms a delicate and dynamic biological system which serves to protect the eye against external insults. Damage to the ocular surface and corneal epithelial stem cells at the limbus from severe cicatricial ocular surface diseases like chemical and thermal burns or Stevens-Johnson Syndrome (SJS), has long posed a major challenge to ophthalmologists.¹⁻³ Limbal stem cell deficiency (LSCD) results in poor corneal epithelial healing, replacement of the corneal epithelium with conjunctiva (conjunctivalization), and corneal scarring that contribute to severe visual loss.

In eyes with unilateral LSCD, autologous transplantation of limbal tissue from the contralateral eye can be performed in an attempt to replace the stem cell population of the diseased eye. In bilateral disease in which there is extensive involvement of both eyes, limbal stem cell transplantation with allogeneic tissue is necessary. However, transplantation of allogeneic tissue necessitates postoperative immunosuppression, bringing about the attendant systemic adverse effects associated with its use. Despite immunosuppression, graft outcomes are still unsatisfactory, as rejection and failure frequently occur.⁴⁻⁷ Subsequent allogeneic transplantation would be associated with even more dismal results. The use of autologous transplantation therefore has significant advantages, as it reduces the risks of transmission of infection or graft rejection and eliminates the need for long-term immunosuppression.

Recently, transplantation of cultivated autologous oral mucosal epithelium has been used in the treatment of LSCD.⁸⁻¹² However, oral mucosa is nonocular tissue, and it retains the characteristics of the tissue of origin. The use of conjunctiva would therefore have obvious advantages for ocular surface epithelial replacement. We have previously demonstrated the effective use of cultivated conjunctival transplantation for conjunctival epithelial replacement in various ocular surface conditions.¹³⁻¹⁷ The use of cultivated conjunctival transplantation for corneal epithelial replacement would be a novel method for treating severe ocular surface disease.

We have described the use of cultivated human conjunctival epithelial cells for corneal resurfacing in a rabbit LSCD model.¹⁸ This is the first study in which relative efficacy of cultivated conjunctival epithelial transplantation was compared with cultivated limbal stem cell transplantation for corneal epithelial replacement. We showed that cultivated conjunctiva epithelial transplantation is a viable alternative to cultivated limbal stem cell transplantation for corneal resurfacing in eyes with LSCD.

From the ¹The Eye and Cornea Transplant Centre, Singapore; the ²Singapore National Eye Centre, Singapore; the ³Department of Ophthalmology, Kyoto Prefectural University of Medicine, Kyoto, Japan; the ⁴Department of Ophthalmology, Yong Loo Lin School of Medicine, National University of Singapore, Singapore; the ⁵Department of Ophthalmology, Tan Tock Seng Hospital, Singapore; and the ⁷Singapore Eye Research Institute, Singapore.

⁵Contributed equally to the work and therefore should be considered equivalent authors.

Submitted for publication January 6, 2009; revised June 8, 2009; accepted November 17, 2009.

Disclosure: L.P.K. Ang, None; H. Tanioka, None; S. Kawasaki, None; L.P.S. Ang, None; K. Yamasaki, None; T.P. Do, None; Z.M. Thein, None; N. Koizumi, None; T. Nakamura, None; N. Yokoi, None; A. Komuro, None; T. Inatomi, None; M. Nakatsukasa, None; S. Kinoshita, None

Corresponding author: Shigeru Kinoshita, Kyoto Prefectural University of Medicine, Department of Ophthalmology, Kawaramachi-Hirokoji, Kamigyo-ku, Kyoto 602-0841, Japan; shigeruk@koto.kpu-m.ac.jp.

TABLE 1. Summary of Clinical Findings for Eyes Receiving Cultivated HCjE, HCE, and Denuded AM Transplants

Treatment Groups	Epithelial Integrity <i>n</i> (%)	Corneal Haze <i>n</i> (%)	Corneal Neovascularization <i>n</i> (%)
Group 1: HCjE transplant (<i>n</i> = 6)	4 (66.7), no defect 2 (33.3), grade 1 defect	4 (66.7), clear 2 (33.3), grade 1 haze	2 (33.3), not significant 2 (33.3), grade 1 1 (16.7), grade 2 1 (16.7), grade 3
Group 2: HCE transplant (<i>n</i> = 6)	4 (66.7), no defect 2 (33.3), grade 1 defect	5 (83.3), clear 1 (16.7), grade 1 haze	3 (50), not significant 1 (16.7), grade 1 2 (33.3), grade 2
Group 3: Denuded AM transplant (<i>n</i> = 6)	2 (33.3), no defect 2 (33.3), grade 1 defect 2 (33.3), grade 4 defect	1 (16.7), clear 5 (83.3), grade 1 haze	1 (16.7), grade 2 5 (83.3), grade 4

MATERIALS AND METHODS

All experimental procedures performed conformed to the ARVO Statement for the Use of Animals in Ophthalmic and Vision Research and were approved by the Committee for Ethical Issues on Human Research of Kyoto Prefectural University of Medicine. Normal human conjunctival epithelial (HCjE) tissues were obtained from patients with conjunctivochalasis who had given informed consent, and human amniotic membranes (AMs) were obtained from consenting mothers at the time of cesarean section. Normal human corneal epithelia (HCE) were obtained from human corneoscleral rims from the Northwest Lion Eye Bank (Seattle, WA).

Preparation of Human Amniotic Membranes

In accordance with the tenets of the Declaration of Helsinki, human placentas were obtained from mothers who had undergone cesarean section and whose test results were negative for hepatitis B and C, syphilis, and human immunodeficiency virus. The membranes were washed with sterile phosphate-buffered saline (PBS) to remove the blood clots and the HAM was peeled away from the chorion and flattened, with the stromal side on a sterilized nitrocellulose filter paper (Millipore, Bedford, MA). The paper with adherent HAM was then stored in 50% DMEM and 50% glycerol (Invitrogen-Gibco, Rockville, MD) at -80°C . Immediately before use, the amniotic membrane was thawed, rinsed with sterile PBS, and incubated in 0.02% EDTA solution (Nakalai Tesque, Kyoto, Japan) for 2 hours, followed by gentle scraping to remove any remaining amniotic epithelial cells.

Ex Vivo Expansion of Conjunctival and Corneal Epithelial Cells on HAM

Corneal and conjunctival epithelial cells were cocultured with mitomycin C (MMC)-treated 3T3 fibroblasts (NIH 3T3; American Type Culture Collection, Manassas, VA). Confluent 3T3 fibroblasts were incubated with 4 mg/mL of MMC for 2 hours at 37°C under 5% carbon dioxide. These were then trypsinized and plated onto plastic dishes with a density of 2×10^4 cells/cm². Denuded HAM (basement membrane-side up) was placed on the porous support membrane (Millipore Corp., Bedford, MA). The membrane was then introduced into wells of a six-well culture plate containing mitomycin-treated 3T3 feeder cells to achieve a dual-chamber culture.

The corneoscleral rims and the conjunctival epithelia were first incubated at 37°C for 1 hour with 1.2 IU dispase (Roche, Tokyo, Japan). The purpose for using dispase was to facilitate separation of epithelial cells from the underlying stromal tissue, so as to promote the outgrowth of epithelial cells on HAM.¹⁹ The epithelium was then removed from the underlying stroma by mechanical scraping and further dissociation with 0.1% trypsin-EDTA. Epithelial cells from the limbal and peripheral corneal region were separated from the underlying stroma carefully. After cell separation, the human conjunctival and corneal epithelial cells were then seeded onto the AM at a density

of 1×10^5 cells/cm² in defined keratinocyte-SFM (Invitrogen, Tokyo, Japan) containing 2% FBS.

On confluence (6–8 days), the epithelial cells were exposed to 7 days of high-calcium conditions (1:1 mixture of defined keratinocyte-SFM containing 2% FBS and DMEM/F12 containing 10% FBS) to promote differentiation and stratification. These conjunctival and corneal equivalents were air lifted for 7 days, to allow further stratification and differentiation of the epithelial cells. Air-lifting was performed by lowering the level of medium to the level of the membrane. Close monitoring of the fluid level was performed twice daily to ensure that the desired level of medium was maintained.

All cultures were incubated at 37°C in a 5% CO₂-95% air incubator, with medium changed every 1 to 2 days. The cultures were monitored under an inverted phase-contrast microscope (Axiovert; Carl Zeiss Meditec, Oberkochen, Germany).

Transplantation of Cultivated Conjunctival and Corneal Epithelial Cells

Total LSCD was created in 18 Japanese white rabbit eyes by surgically removing the entire corneal epithelium by superficial keratectomy. To ensure complete removal of the limbal epithelium, we surgically excised the entire limbal epithelium and surrounding conjunctival tissue up to 2 mm beyond the limbus from one eye, down to the bare sclera.

The rabbits were then divided into three treatment groups (Table 1): group 1, cultivated human conjunctival epithelial (HCjE) transplantation (*n* = 6); group 2, cultivated human corneal epithelial (HCE) transplantation (*n* = 6); and group 3, denuded human amniotic membrane transplantation (*n* = 6).

The epithelial sheets and HAM were transplanted onto the denuded corneal surface to completely cover the resected area and sutured with 10-0 nylon sutures. The graft was covered with a therapeutic soft contact lens and secured with four peripheral anchoring sutures. A total tarsorrhaphy was performed with 6-0 nylon sutures.

After surgery, the rabbits were treated with topical antibiotics of 0.3% ofloxacin ointment (Santen Pharmaceutical Co., Ltd, Osaka, Japan), triamcinolone acetonide 0.2 mL injected subconjunctivally (Bristol Myers Squibb Co., Tokyo, Japan), and systemic antibiotics (10 mg gentamicin/rabbit, delivered intramuscularly; Nacalai Tesque, Inc.). They also received a daily IM injection of 0.2 mg/kg of the immunosuppressant agent FK506 (Astellas Co., Ltd., Tokyo, Japan) to inhibit a possible xenogenic reaction or nonspecific inflammation.

Slit Lamp Examination

The ocular surfaces of the rabbits were examined, stained with fluorescein, and photographed with a slit lamp biomicroscope (SL-1600; Nidek Co., Ltd., Aithi, Japan) on the day of transplantation and on the 14th postoperative day. The main outcome measures were graded as follows.

Epithelial Integrity. Grade 0, no epithelial defect; 1, less than or equal to one fourth of the corneal surface; 2, from one fourth to one